nature geoscience

Article

https://doi.org/10.1038/s41561-023-01320-1

Southeast Asian ecological dependency on Tibetan Plateau streamflow over the last millennium

Received: 28 March 2023

Accepted: 6 October 2023

Published online: 13 November 2023

Check for updates

Feng Chen[1,2,18] ✉, Wenmin Man[3,18], Shijie Wang[1,2], Jan Esper[4,5], David Meko[6], Ulf Büntgen[5,7,8,9], Yujiang Yuan[10], Martín Hadad[11], Mao Hu[1,2], Xiaoen Zhao[1,2], Fidel A. Roig[12,13], Ouya Fang[14], Youping Chen[1], Heli Zhang[1,10], Huaming Shang[10], Shulong Yu[10], Xian Luo[1], Daming He[1] ✉ & Fahu Chen[15,16,17] ✉

The great river systems originating from the Tibetan Plateau are pivotal for the wellbeing of more than half the global population. Our understanding of historical ranges and future changes in water availability for much of Southeast Asia is, however, limited by short observational records and complex environmental factors. Here we present annually resolved and absolutely dated tree ring-based streamflow reconstructions for the Mekong, Salween and Yarlung Tsangpo rivers since 1000 CE, which are supplemented by corresponding model projections until 2100 CE. We show a significant positive correlation between streamflow and dry season vegetation indices over the Indochinese Peninsula, revealing the importance of the Tibetan Water Tower for the functioning and productivity of ecological and societal systems in Southeast Asia. The streamflow variability is associated with low-frequency sea-surface temperature variability in the North Atlantic and North Pacific. We find that streamflow extremes coincide with distinct shifts in local populations that occurred during medieval times, including the occupation and subsequent collapse of Angkor Wat from the eleventh to the sixteenth century. Finally, our projections suggest that future streamflow changes will reach, or even exceed, historical ranges by the end of this century, posing unprecedented risks for Southeast Asia.

The Tibetan Plateau is often referred to as the Asian water tower since the glacially fed rivers that flow from the plateau are a primary source of water for much of south and Southeast Asia, and plays an important role in linking hydrological cycles with ecological and socioeconomic systems in these great river basins[1–8]. The relationships between the upstream water resources and the diverse and widely distributed populations that depend on these resources across the great Asian transboundary river basins (that include the Mekong, Salween and Yarlung Tsangpo (the upper Brahmaputra) rivers) may vary on the different time scale; however, these relationships are not yet fully understood[9–11]. Although modern instrumental records of regional streamflow offer some insight into the relationships between contemporary local populations and water resources variability, the lack of reliable historical records extending beyond the instrumental period has resulted in debates about the role of past water resources variability played in the rise and decline of the indigenous civilizations that previously occupied the river basins of Southeast Asia[12–15]. Climatologists, historians and archaeologists have examined the direct and indirect

A full list of affiliations appears at the end of the paper. ✉e-mail: feng653@163.com; dmhe@ynu.edu.cn; fhchen@itpcas.ac.cn

importance that climatic and environmental factors have on affecting societal changes within Asian transboundary river basins, with particular emphasis given to the influence of the monsoon system[12–19]. Since the eleventh century CE, several culturally distinct civilizations have arisen in Southeast Asia, such as the Khmer Empire, which controlled a large fraction of the Indochinese Peninsula. These states depended heavily on vast and complex rice-cultivation systems supported by monsoon precipitation and freshwater from streams and rivers[20,21]. Previous studies also have examined how hydroclimate more broadly influenced the abandonment of Angkor Wat[17]. However, in addition to summer monsoon[16,17], the water resources of major river basins in Southeast Asia are influenced by the Tibetan Water Tower[2,5], which provides water from the melting of snow and glaciers. Except for the droughts that may arise from monsoon instability, Southeast Asian societies were, are and will continue to be vulnerable to the hydrologic variability of the Tibetan Water Tower, since potential instabilities in that source may trigger either droughts or flooding.

To understand the influence of changes in hydroclimate variability on human populations, several hydroclimate simulations have been conducted for this region[22–30]. However, the complex topography and associated atmospheric dynamics of High Asia make it difficult for climatic and hydrological models to accurately simulate natural streamflow variability or contextualize past changes, especially considering how anthropogenic forcings influence current and predicted patterns[22–32]. These limitations cause great uncertainty in the prediction of water resource changes under different future climate change scenarios[26–30]. Reliable streamflow reconstructions can be used to validate model outputs and estimate the potential streamflow variability under different climate conditions. Additionally, a proxy-based, long-term hydrological perspective is needed to validate the model outputs[33–37]. Thus, improving knowledge regarding long-term streamflow changes is of great importance for future predictions of the regional hydrological cycle. In this Article, we present a well-dated and annually resolved 1,000-year-long September–July streamflow reconstructions of the Mekong, Salween and Yarlung Tsangpo rivers, and indicate that the impact of streamflow from the Tibetan Plateau on the Southeast Asian ecological and societal systems. A comparison between our dendrochronology-based streamflow reconstructions and an ensemble of state-of-the-art Community Earth System Model (CESM)[38] simulations permits the identification of the mechanisms that impact these streamflow changes. Additionally, we consider various shared socioeconomic pathway (SSP 2-4.5 and SSP 5-8.5) scenarios to describe different future streamflow change projections. This new record allows us to investigate the linkage between water supply from the Tibetan Plateau and Southeast Asian economies and societies over the past millennium.

Streamflow reconstruction derived from tree rings

The Mekong, Salween and Yarlung Tsangpo catchments have similar hydroclimatic conditions, and this similarity supports the comprehensive reconstruction of past streamflow variability using a network of moisture-sensitive tree-ring-width chronologies from southern Tibetan Plateau (Fig. 1a, Supplementary Figs. 1 and 2, and Supplementary Table 1). Instrumental streamflow data and tree-ring radial growth are positively correlated with gridded precipitation, temperature and moisture availability (scPDSI)[39,40], which are obtained from the Climatic Research Unit, East Anglia, United Kingdom (http://www.cru.uea.ac.uk) (Supplementary Figs. 3 and 4). We used the annually resolved tree-ring-width site chronologies from ten sampling sites in the southern Tibetan Plateau that encompassed ~1,000 years to develop an extended September–July streamflow record for the sum of the flows of the Mekong, Salween and Yarlung Tsangpo rivers from 1000 to 2018 CE using a nested principal component regression method (Methods). The reconstruction accounts for 42.0–61.0% of the instrumental streamflow variance during the 1961–2004 CE calibration period (Fig. 1b,c and Supplementary Table 2). This indicates that this tree-ring record provides a 1,000-year perspective on the water supply of the Tibetan Plateau to Southeast Asia (Fig. 1b). The long-term means of the streamflow reconstruction is $1{,}576.5 \times 10^8$ m^3 for the period 1000–2018 CE. The reconstructed streamflow was generally low from ~1000 to 1040 CE, but the strongest and most persistent increase (+3.5%, $1{,}631.7 \times 10^8$ m^3) over the last 1,000 years occurred from ~1050 to 1199 CE. A major decrease in streamflow occurred from the early thirteenth century to the early sixteenth century, with exceptionally low flows from ~1280 to 1330 CE (−2.1%, $1{,}544.2 \times 10^8$ m^3), ~1360 to 1409 CE (−2.2%, $1{,}541.2 \times 10^8$ m^3) and ~1420 to 1509 CE (−4.3%, $1{,}509.4 \times 10^8$ m^3). Although the drought during the fourteenth century has been referenced in contemporary national chronicles of Southeast Asian countries[14,15,17], little attention has been given to the decrease in river flow that occurred on the southern Tibetan Plateau from the early thirteenth century to the early sixteenth century, though other records suggest that these decreasing trends may have been widespread in High Asia and may even have extended northwards into central China[41–44] (Fig. 2). Inter-annual to multidecadal variations in streamflow continued until the late twentieth-century warm period, when streamflow began an increasing trend (+5.8%, $1{,}668.9 \times 10^8$ m^3) that has continued since the 1990s. Moreover, the running variance of the reconstructed streamflow indicates a continuously upward trend (Fig. 1d), indicating streamflow has become more variable in these river basins.

No significant correlations with Normalized Difference Vegetation Index (NDVI)[45] occurred in the Indochinese Peninsula during the monsoon season. However, together with the beginning of the dry season, the correlations between the streamflow reconstruction and the NDVI in the Indochinese Peninsula gradually increased, with the highest correlation ($r = 0.55$, $P < 0.01$) observed for reconstructed streamflow and mean April–May NDVI of following year (Fig. 3a,b).

Streamflow links to large-scale atmospheric circulation

Our streamflow reconstruction is positively correlated with gridded instrumentally derived sea-surface temperatures (SSTs)[46] of the North Atlantic and North Pacific Oceans from 1870 to 2018, with a strong trend towards high streamflow in the late twentieth century (Fig. 4a and Supplementary Fig. 5). This suggests possible teleconnections between the regional streamflow and Atlantic multidecadal variability (AMV)[47] and Pacific Decadal Oscillation (PDO)[48]. The evidence from the Community Earth System Model Last Millennium Ensemble (CESM-LME) and climate reconstructions indicate that the AMV[47] and PDO[49] may account for a minor but potentially important portion of the explained variance in regional streamflow and climate (Fig. 4b, Supplementary Figs. 6 and 7, and Supplementary Table 3). We also observed significant correlations between the simulated streamflow and simulated temperature in the CESM-LME outputs, and the streamflow reconstruction also corresponded well ($r_{1000–2018} = 0.49$, $P < 0.01$) with the temperature changes on the eastern Tibetan Plateau, which have a robust in-phase relationship with the Atlantic multidecadal oscillation(AMO) during the last millennium (Fig. 4c,d), indicating the important role of temperature changes in affecting regional streamflow[50,51]. A positive PDO phase weakens the Walker circulation and results in reduced convective activity and precipitation over the Indo-Pacific Warm Pool. This decreased latent heating further leads to a weakened South Asian monsoon via the baroclinic Rossby wave trains emanating from the western Pacific and, hence, to a reduction in the amount of water vapour transported to the eastern Tibetan Plateau (Fig. 4e). At the same time, positive AMV thus strengthens the westerly jet along the northern slopes of the Tibetan Plateau, thereby promoting increased precipitation across the southeastern Tibetan Plateau (Fig. 4f). Thus, past streamflow variations derived from the CESM simulations appear not to be forced directly—that is, they arise as a feature of changes in the internal regional climate factors (for example, temperature and precipitation) that linked with AMO and

https://doi.org/10.1038/s41561-023-01320-1

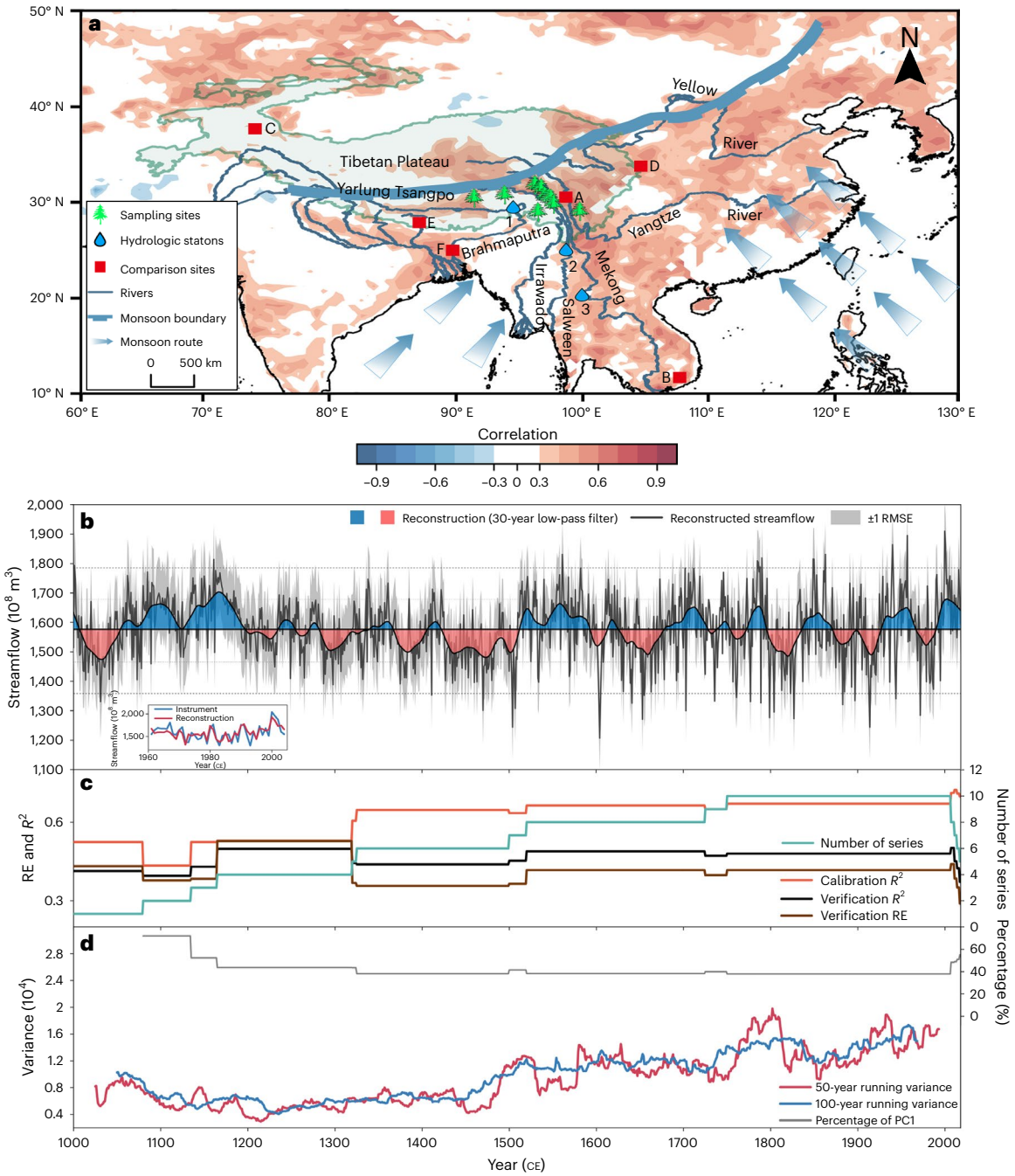

Fig. 1 | Spatio-temporal aspects of streamflow reconstruction. **a**, Map showing the study area and location of tree-ring sites and streamflow gauges in the Mekong, Salween and Yarlung Tsangpo basins. Background colours highlight correlations ($P < 0.05$, two tailed) between streamflow reconstruction and gridded NDVI data of the April–May dry season from 1982 to 2019. The numbers 1, 2 and 3 denote the locations of Nuxia, Daojieba and Chiang Saen hydrological stations, respectively. The regions A, B, C, D, E and F indicate the comparison sites of southeastern Tibetan Plateau[41], southern Vietnam[17], Karakoram Mountains[42], Wanxiang Cave[43], Dasuopu[44] and Brahmaputra River[36], respectively. **b**, The full reconstruction back to 1000 CE at annual resolution and 30-year low-pass-filtered. The grey color band around the reconstruction indicates the root-mean-square error (RMSE). The inset figure shows comparison between actual and estimated streamflow for the period 1960–2004. **c**, Explained variance (R^2), RE and numbers of series for each segment. **d**, Fifty- and 100-year running bi-weighted variance for the streamflow reconstruction, and the percentage total variance of the first principal component (PC1) of the tree-ring-width chronologies.

PDO (Supplementary Figs. 8 and 9), and as a result, the simulations and reconstruction are uncorrelated on both the inter-annual and decadal scales throughout the last millennium.

Projections of future streamflow

The decadal changes in the simulated streamflow were affected by internal variabilities and anthropogenic forcing during the recent warm period 1850–2005, of which the most significant forcing factors in this interval were anthropogenic aerosols and the AMV, which contributed 31.6% and 20.0% of the streamflow variability, respectively (Supplementary Fig. 9). Increased streamflow over the eastern Tibetan Plateau was also simulated by the ensemble mean of the Coupled Model Intercomparison Project version 6 (CMIP6) models during the high SST periods 1930–1950 and 1980–2005[46] (Fig. 4g and

https://doi.org/10.1038/s41561-023-01320-1

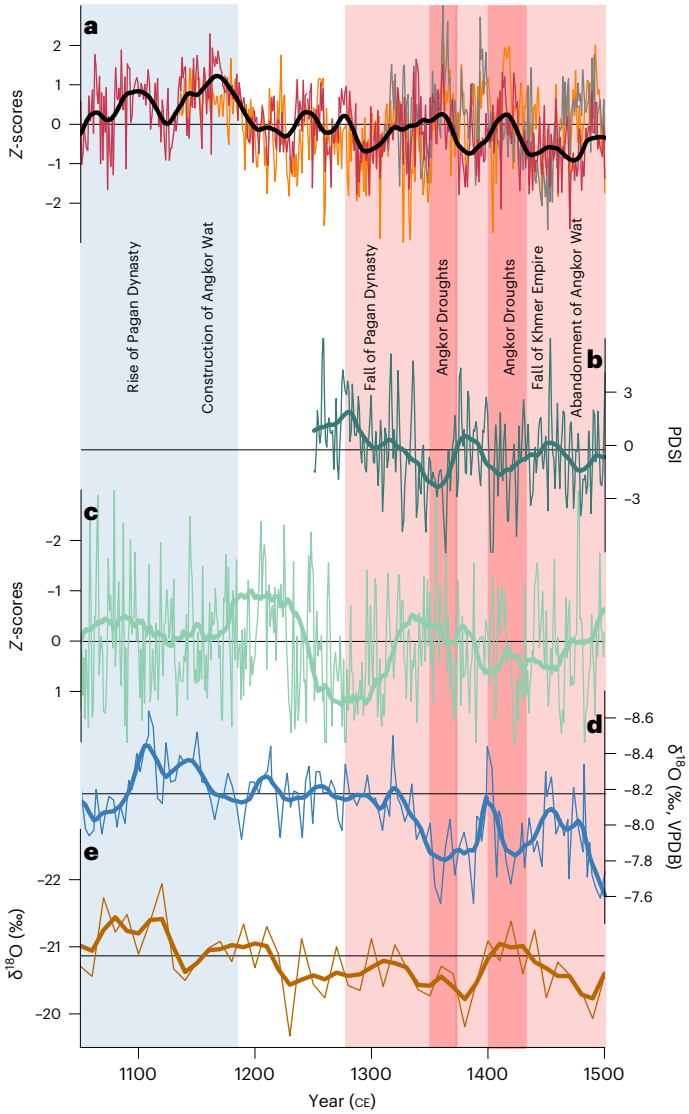

Fig. 2 | Comparison of the reconstructed streamflow with regional palaeoclimate records from 1050 to 1500 CE. a, Our streamflow (with bold curve, 30-year low-pass filter), the drought reconstruction for the southeastern Tibetan Plateau[41] ($r_{1135–2010}$ = 0.67, P < 0.01, two tailed) and reconstructed Brahmaputra River discharge[36] ($r_{1309–2004}$ = 0.39, P < 0.01, two tailed). **b**, Drought reconstruction (with bold curve, 30-year low-pass filter) from the Bidoup Nui Ba National Park (BDNP) in the tropical southern Vietnam[17]. **c**, Tree-ring $\delta^{18}O$ record (with bold curve, 100-year Savitzky–Golay filter) from the Karakoram Mountains[42] in northern Pakistan. **d**, Speleothem $\delta^{18}O$ record (with bold curve, 10-year low-pass filter) from Wanxiang Cave[43] in China. VPDB, Vienna Pee Dee belemnite. **e**, Dasuopu $\delta^{18}O$ ice core record (with bold curve, 5-year low-pass filter)[44]. The locations of the compared series are shown in Fig. 1a.

Supplementary Fig. 10). Future streamflow projections from CMIP6 reveal a persistent externally driven increasing trend from the 2030s to the end of the twenty-first century. Whereas streamflow remains relatively constant from the 2060s to the 2090s considering the SSP2-4.5 scenario, the SSP5-8.5 scenario returns a persistent and increased trend throughout the twenty-first century (Fig. 4g). This trend can also be observed in the comparison of the kernel density profile of streamflow projections under different scenarios for the 2019–2100 period with the kernel density profiles of both the instrumental period of 1961–2004 and the entire period of 1000–2018 (Fig. 4h).

Streamflow and historical societal changes in Southeast Asia

The downstream reaches of the Mekong, Salween and Yarlung Tsangpo rivers comprise the most densely populated region on Earth. Although these catchment areas experience abundant precipitation, seasonal and inter-annual variability of streamflow is controlled by the Asian summer monsoon[16,17,52,53]. Since these major rivers are critical for alleviating water supply concerns[8,54,55], it is critical to understand their long-term variability. The new streamflow reconstruction presented herein places variability into a long-term, millennium-scale context and provides the information needed to analyse the changing relationships between socioeconomic development in Southeast Asia and the water supply from the Tibetan Plateau both before and during the most recent interval of anthropogenic-induced climate alteration. Coinciding with the general decline in streamflow since the early thirteenth century, medieval empires began to fragment, the political landscape of the Indochina Peninsula was continuously reformed, and prototypes of the modern states of Thailand and Laos began to develop[56–59].

The inter-regional streamflow reconstruction presented here reveals a strong increase in flow rate from the 1050s to the 1190s (Fig. 2). This increase was parallelled by rapid socioeconomic and cultural growth[56–59], including (1) the rise of the Bagan Dynasty and the related unification of Burma from the 1050s to the 1070s CE, (2) the rise of the Khmer Empire and construction of Angkor Wat (1110s to 1150s CE), and (3) the conquest of the Champa in the mid-twelfth century. A trend of decreasing streamflow from the early thirteenth century to the late fifteenth century was accompanied by the intervention of external forces and several major challenges to the socioeconomic, political and cultural systems of Southeast Asia. From 1280 to 1340 CE, the streamflow trend coincided with a major crisis in the Pagan Dynasty, as evidenced by the Mongol invasion in 1287 (ref. 59). This crisis was characterized by economic dislocation, political turmoil and the division of Myanmar. The most prolonged low-streamflow period of the past ~1,000 years, from 1360 to 1500 CE, coincided with collapse of the Khmer Empire and slow abandonment of Angkor Wat[17,56,59]. Through the conquest of the Kingdom of Champa in the low streamflow period 1470s, the territory of the later Lê Dynasty was expanded, which approached the size of modern Vietnam[56,58].

Low and high streamflow periods of greater magnitude and duration than those in the instrumental record occurred during the period 1050s to 1510s. This increasing variability probably affected not only rice cultivation, but also local fish harvest and, thereby, the food provisions of the human population of Southeast Asia[25] (Fig. 3c). This conclusion is reinforced by the positive correlations identified between our streamflow reconstruction data and the dry-season NDVI, an indirect indicator of grain yield. Whereas the high streamflow probably facilitated larger fish harvests[60] (Supplementary Fig. 11) and supported the economic and political strengths required to implement major construction projects, such as Angkor Wat and Pagan City, the low streamflow measured from the early thirteenth century to the late fifteenth century were largely characterized by the limited fish stock associated with the demise of the Khmer Empire[61] and the abandonment of Angkor Wat, which did not occur rapidly but rather was an extended process[20,62,63]. This is because, even though prosperous nations may be more resilient and potentially more adaptive to climatic extremes, the influence of long-term adverse environmental factors may affect this resilience, and hydrological extremes may trigger gradual societal changes[61–63].

Although archaeological evidence indicates that already-fragile water systems, coupled with abrupt climatic variation, contributed to the demise of the city[64], the role of streamflow variation in this process has not been revealed. Our new streamflow reconstruction suggests that, among the myriad stressors impacting the Khmer Empire (for example, summer monsoon failures and societal and political issues)[17], their decline may also have been influenced by a long-term, ~200-year

https://doi.org/10.1038/s41561-023-01320-1

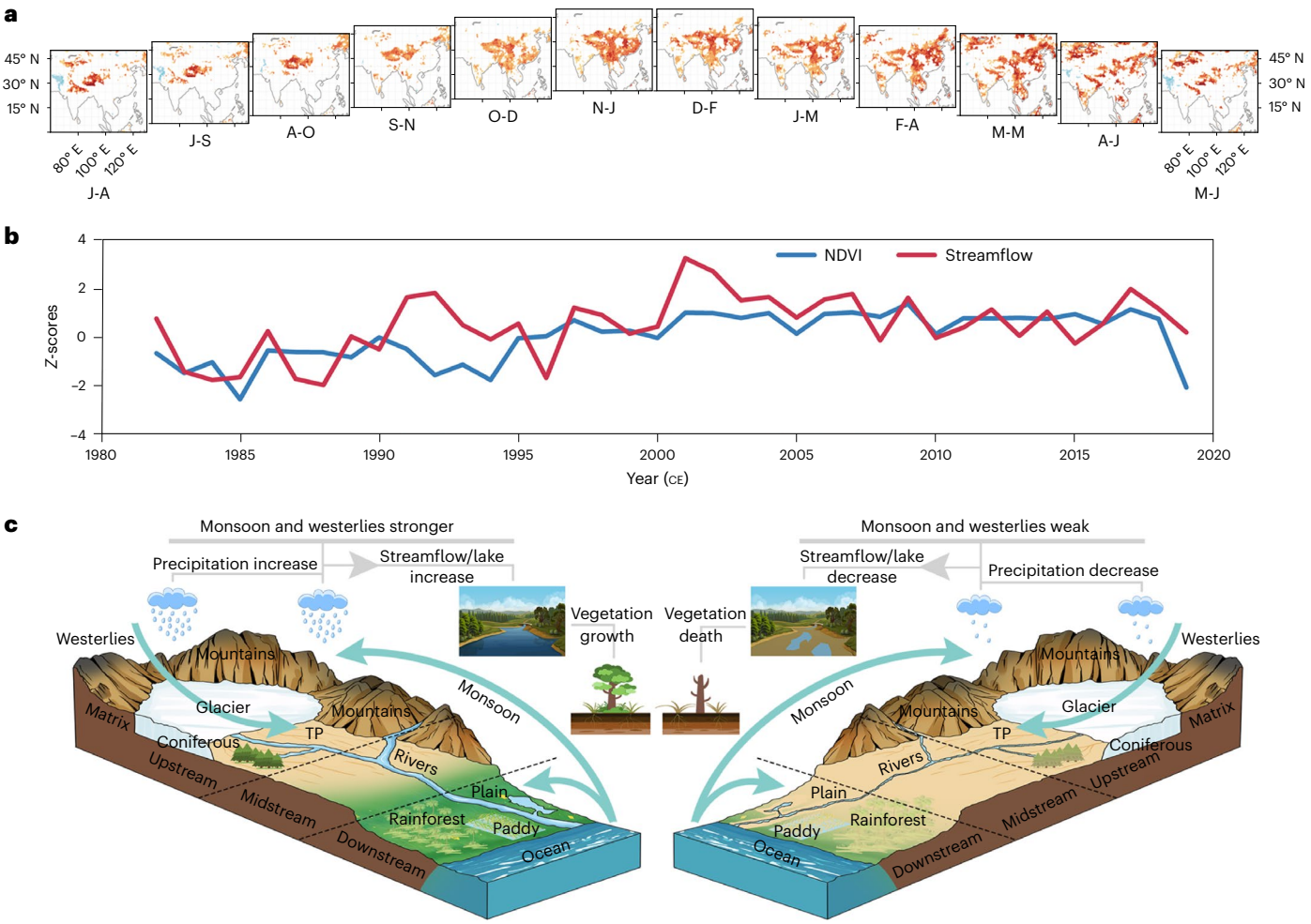

Fig. 3 | Links of reconstructed streamflow to vegetative cover. a, Correlations of the streamflow reconstruction versus gridded 3-monthly NDVI data[45] from current June to July of the following year during the period 1982–2019. **b**, Instrumental NDVI versus reconstructed September–July streamflow, 1982–2019 ($r = 0.55$, $P < 0.01$, two tailed). **c**, Conceptual models of the watershed system, including glaciers, rivers, irrigation systems, lakes and forests, and dominating weather patterns during periods of high (top) and low streamflow (bottom).

interval of limited streamflow from the Tibetan Plateau. However, this argumentation does not suggest that hydroclimate variability alone is the sole driver of societal evolution in major river basins, but instead posits that significant long-term deviations and changes in the frequency of climate extremes need to be considered in addition to economic, ethnic, religious and cultural factors, particularly in Southeast Asia due to its complex multicultural and religious background.

Connections between streamflow and climatic change

Rapid increases in streamflow of the three transboundary rivers on the southern Tibetan Plateau beginning in the 1990s are rare but not without precedent over the last ~1,000 years. Comparison with regional tree-ring-based temperature reconstructions reveals the importance of this variable for the snow and glacier-derived meltwater amounts leaving the Tibetan Plateau (Fig. 4c,d)[5,65]. Our reconstruction shows that the amplitudes of streamflow events during the Medieval Climate Anomaly and Little Ice Age (LIA) exceeded those within the instrumental streamflow record, and this substantial difference was also probably related to the melting of snow and glacier ice associated with remote but persistent atmospheric circulation anomalies, such as the negative AMO phase during the Little Ice Age[66,67] (Fig. 4e,f). This pattern has reversed during the current warm period. This suggests that streamflow of the river basins studied in this work is controlled by the complex feedback effects among the ocean, atmosphere and land that may create variabilities and instabilities in inter-regional hydroclimatic conditions, such as variabilities in the expected increases in rainfall and evaporation, as well as in glacier responses to rising temperatures[2]. Our study found that the AMV and PDO are important internal modes that contribute to the streamflow during the past millennium. Considering the persistence of interdecadal oscillations, improving the predictive skill for internal variability modes, including the AMV and PDO, is expected to improve the streamflow predictions at decadal scales. Thus, our study calls for further understanding and prediction of the near-term evolutions of the AMV/PDO, and other decadal modes of internal variability to improve the High Asian streamflow projection under global warming.

Streamflow variability and the related changes in vegetation productivity have severe impacts on the natural and agricultural ecosystems of Southeast Asia. The socioeconomic perspectives on past extreme streamflow conditions reveal that past societies had some degree of vulnerability to changes in the water supply from the Tibetan Plateau. Understanding this demonstrated historical link between the water supply leaving the Tibetan Plateau and the socioeconomic development of Southeast Asia may help to strengthen scientific and economic cooperation among the dominant cultural groups within the basins and promote a transnational sustainable development plan. The rising streamflow trend identified herein will probably

https://doi.org/10.1038/s41561-023-01320-1

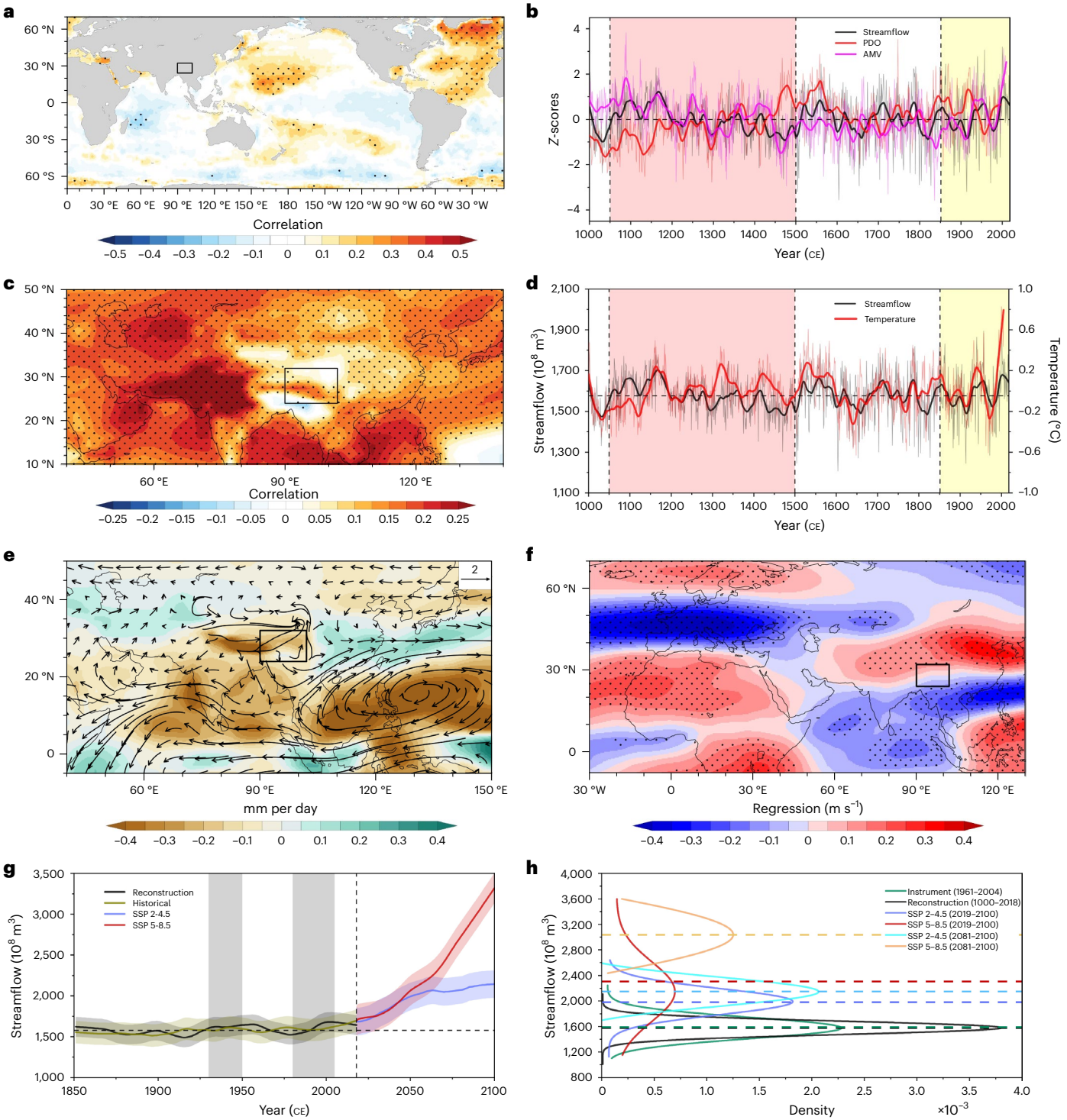

Fig. 4 | Relationship of reconstructed streamflow with simulated and observed climate series and indices of the climate system. a, Spatial correlation map of the reconstructed streamflow with September–July SST[46] from 1870 to 2018. Dots denote 95% significance levels. **b**, Comparison of the reconstructed streamflow with AMV[47] and PDO[49] during the last millennium. Thick lines are 30-year low-pass filter results, and thin lines are the original series. **c**, Spatial correlation pattern of the CESM-LME simulated runoff and temperature[38] during the last millennium. Dots denote 95% significance levels. **d**, Comparison of the reconstructed streamflow with eastern Tibetan Plateau temperature during the last millennium[50]. **e**, Spatial precipitation differences (shading, mm per day) and 500 hPa water vapour transport (vectors, kg m^{-1} s^{-1}) between the positive PDO composite and the negative PDO compos based on the CESM-LME simulation during the last millennium. **f**, Patterns of the 200 hPa zonal wind (shading; m s^{-1}) associated with the AMV index based on the CESM-LME simulation. Stippling indicates that the regression coefficients are significant at the 1% level according to the Student's *t*-test. **g**, Time series of the 30-year running mean of the September–July streamflow anomaly (mm per month) during 1850–2100 relative to the reconstruction mean (1000–2018) in the reconstruction (black) and historical simulations (green), and under SSP2-4.5 (blue) and SSP5-8.5 scenarios (red). Lines denote the ensemble mean, and the shadings denote the ensemble spread (±1 s.d.). The horizontal dashed line denotes the reconstruction mean. **h**, Kernel probability density estimate of the regional streamflow during the reconstruction period (1000–2018) (black), the instrumental period (1961–2004) (green) and the future (2019–2100) under SSP2-4.5 (blue) and SSP5-8.5 scenarios (red). Horizontal dashed line denotes the respective mean values.

continue throughout the coming decades, potentially reaching or even exceeding the high levels shown by the reconstruction during the Medieval era. However, this increase will probably not compensate for the rapid socioeconomic and demographic growth in Southeast Asia, which means that water scarcity problems will probably continue to intensify. The various nations along these river basins therefore need strengthened cooperation to improve water preservation strategies and maintain their water resources. Moreover, water resource allocation is complicated by uncertainties in simulation results and by the self-interest of individual countries, which hinders the formulation of effective adaptation strategies. Addressing these uncertainties should remain a priority to improve future hydrological simulations that can inform decisions regarding water use and allocation.

Online content

Any methods, additional references, Nature Portfolio reporting summaries, source data, extended data, supplementary information, acknowledgements, peer review information; details of author contributions and competing interests; and statements of data and code availability are available at https://doi.org/10.1038/s41561-023-01320-1.

References

1. Milly, P. C., Dunne, K. A. & Vecchia, A. V. Global pattern of trends in streamflow and water availability in a changing climate. *Nature* **438**, 347–350 (2005).
2. Yao, T. et al. Recent Third Pole's rapid warming accompanies cryospheric melt and water cycle intensification and interactions between monsoon and environment: multidisciplinary approach with observations, modeling, and analysis. *Bull. Am. Meteorol. Soc.* **100**, 423–444 (2019).
3. Brun, F., Berthier, E., Wagnon, P., Kääb, A. & Treichler, D. A spatially resolved estimate of High Mountain Asia glacier mass balances from 2000 to 2016. *Nat. Geosci.* **10**, 668–673 (2017).
4. Dehecq, A. et al. Twenty-first century glacier slowdown driven by mass loss in High Mountain Asia. *Nat. Geosci.* **12**, 22–27 (2019).
5. Immerzeel, W. W., Van Beek, L. P. & Bierkens, M. F. Climate change will affect the Asian water towers. *Science* **328**, 1382–1385 (2010).
6. Kraaijenbrink, P. D. A., Bierkens, M. F. P., Lutz, A. F. & Immerzeel, W. W. Impact of a global temperature rise of 1.5 degrees Celsius on Asia's glaciers. *Nature* **549**, 257–260 (2017).
7. Bolch, T. Hydrology: Asian glaciers are a reliable water source. *Nature* **545**, 161–162 (2017).
8. Lutz, A. F., Immerzeel, W. W., Shrestha, A. B. & Bierkens, M. F. P. Consistent increase in High Asia's runoff due to increasing glacier melt and precipitation. *Nat. Clim. Change* **4**, 587–592 (2014).
9. Chellaney, B. *Water: Asia's New Battleground* (Georgetown Univ. Press, 2011).
10. Liang, Y., Chen, Y., Chen, F. & Zhang, H. Possible role of the regional NDVI in the expansion of the Chiefdom of Lijiang during the Ming Dynasty as reflected by historical documents and tree rings. *Weather Clim. Soc.* **14**, 1107–1118 (2022).
11. Wang, T. et al. Atmospheric dynamic constraints on Tibetan Plateau freshwater under Paris climate targets. *Nat. Clim. Change* **11**, 219–225 (2021).
12. Lieberman, V. & Buckley, B. The impact of climate on Southeast Asia, circa 950–1820: New findings. *Mod. Asian Stud.* **46**, 1049–1096 (2012).
13. Buckley, B. M., Fletcher, R., Wang, S. Y. S., Zottoli, B. & Pottier, C. Monsoon extremes and society over the past millennium on mainland Southeast Asia. *Quat. Sci. Rev.* **95**, 1–19 (2014).
14. Day, M. B. et al. Paleoenvironmental history of the west Baray, Angkor (Cambodia). *Proc. Natl Acad. Sci. USA* **109**, 1046–1051 (2012).
15. Fletcher, R., Buckley, B. M., Pottier, C. & Wang, S. Y. S. in *Megadrought and Collapse: From Early Agriculture to Angkor* (ed. Weiss, H.) 275–314 (2017).
16. Cook, E. R. et al. Asian monsoon failure and megadrought during the last millennium. *Science* **328**, 486–489 (2010).
17. Buckley, B. M. et al. Climate as a contributing factor in the demise of Angkor, Cambodia. *Proc. Natl Acad. Sci. USA* **107**, 6748–6752 (2010).
18. Chen, F. et al. Ecological and societal effects of Central Asian streamflow variation over the past eight centuries. *NPJ Clim. Atmos. Sci.* **5**, 1–8 (2022).
19. DeMenocal, P. B. Cultural responses to climate change during the late Holocene. *Science* **292**, 667–673 (2001).
20. Lieberman, V. Charter state collapse in Southeast Asia, ca. 1250–1400, as a problem in regional and world history. *Am. Hist. Rev.* **116**, 937–963 (2011).
21. Fox, J. & Ledgerwood, J. Dry-season flood-recession rice in the Mekong Delta: two thousand years of sustainable agriculture? *Asian Perspect.* **38**, 37–50 (1999).
22. Grill, G. et al. Mapping the world's free-flowing rivers. *Nature* **569**, 215–221 (2019).
23. Gao, J., Yao, T., Masson-Delmotte, V., Steen-Larsen, H. C. & Wang, W. Collapsing glaciers threaten Asia's water supplies. *Nature* **565**, 19–21 (2019).
24. Schmitt, R. J., Bizzi, S., Castelletti, A., Opperman, J. J. & Kondolf, G. M. Planning dam portfolios for low sediment trapping shows limits for sustainable hydropower in the Mekong. *Sci. Adv.* **5**, eaaw2175 (2019).
25. Sabo, J. L. et al. Designing river flows to improve food security futures in the Lower Mekong Basin. *Science* **358**, eaao1053 (2017).
26. Fendorf, S., Michael, H. A. & van Geen, A. Spatial and temporal variations of groundwater arsenic in South and Southeast Asia. *Science* **328**, 1123–1127 (2010).
27. Hackney, C. R. River bank instability from unsustainable sand mining in the lower Mekong River. *Nat. Sustain.* **3**, 1–9 (2020).
28. Pritchard, H. D. Asia's shrinking glaciers protect large populations from drought stress. *Nature* **569**, 649–654 (2019).
29. Veldkamp, T. I. E. et al. Water scarcity hotspots travel downstream due to human interventions in the 20th and 21st century. *Nat. Commun.* **8**, 1–12 (2017).
30. Mekonnen, M. M. & Hoekstra, A. Y. Four billion people facing severe water scarcity. *Sci. Adv.* **2**, e1500323 (2016).
31. Qi, W., Liu, J., Xia, J. & Chen, D. Divergent sensitivity of surface water and energy variables to precipitation product uncertainty in the Tibetan Plateau. *J. Hydrol.* **581**, 124338 (2020).
32. Liu, W. et al. Investigating water budget dynamics in 18 river basins across the Tibetan Plateau through multiple datasets. *Hydrol. Earth Syst. Sci.* **22**, 351–371 (2018).
33. Cook, E. R. et al. Five centuries of Upper Indus River flow from tree rings. *J. Hydrol.* **486**, 365–375 (2013).
34. Chen, F. et al. 500-Year tree-ring reconstruction of Salween River streamflow related to the history of water supply in Southeast Asia. *Clim. Dyn.* **53**, 6595–6607 (2019).
35. Nguyen, H. T., Turner, S. W., Buckley, B. M. & Galelli, S. Coherent streamflow variability in monsoon Asia over the past eight centuries-Links to oceanic drivers. *Water Resour. Res.* **56**, e2020WR027883 (2020).
36. Rao, M. P. et al. Seven centuries of reconstructed Brahmaputra River discharge demonstrate underestimated high discharge and flood hazard frequency. *Nat. Commun.* **11**, 1–10 (2020).
37. Wu, Y. et al. Reconstructed eight-century streamflow in the Tibetan Plateau reveals contrasting regional variability and strong nonstationarity. *Nat. Commun.* **13**, 1–13 (2022).
38. Otto-Bliesner, B. L. et al. Climate variability and change since 850 CE: an ensemble approach with the Community Earth System Model. *Bull. Am. Meteorol. Soc.* **97**, 735–754 (2016).

39. Harris, I., Osborn, T. J., Jones, P. & Lister, D. Version 4 of the CRU TS monthly high-resolution gridded multivariate climate dataset. *Sci. Data* **7**, 1–18 (2020).
40. Ghiggi, G., Humphrey, V., Seneviratne, S. I. & Gudmundsson, L. G-RUN ENSEMBLE: a multi-forcing observation-based global runoff reanalysis. *Water Resour. Res.* **57**, e2020WR028787 (2021).
41. Wang, J., Yang, B. & Ljungqvist, F. C. Moisture and temperature covariability over the Southeastern Tibetan Plateau during the Past Nine Centuries. *J. Clim.* **33**, 6583–6598 (2020).
42. Treydte, K. S. et al. The twentieth century was the wettest period in northern Pakistan over the past millennium. *Nature* **440**, 1179–1182 (2006).
43. Zhang, P. et al. A test of climate, sun, and culture relationships from an 1810-year Chinese cave record. *Science* **322**, 940–942 (2008).
44. Thompson, L. G. et al. A high-resolution millennial record of the South Asian monsoon from Himalayan ice cores. *Science* **289**, 1916–1919 (2000).
45. Vermote, E. & NOAA CDR Program. NOAA Climate Data Record (CDR) of AVHRR Normalized Difference Vegetation Index (NDVI), Version 5. *NOAA* https://doi.org/10.7289/V5ZG6QH9 (2019).
46. Rayner, N. A. A. et al. Global analyses of sea surface temperature, sea ice, and night marine air temperature since the late nineteenth century. *J. Geophys. Res. Atmos.* **108**, D14 (2003).
47. Wang, J. et al. Internal and external forcing of multidecadal Atlantic climate variability over the past 1,200 years. *Nat. Geosci.* **10**, 512–517 (2017).
48. Henley, B. J. et al. A tripole index for the interdecadal Pacific oscillation. *Clim. Dyn.* **45**, 3077–3090 (2015).
49. MacDonald, G. M. & Case, R. A. Variations in the Pacific Decadal Oscillation over the past millennium. *Geophys. Res. Lett.* **32**, L08703 (2005).
50. Wang, J., Yang, B. & Ljungqvist, F. C. A millennial summer temperature reconstruction for the eastern Tibetan Plateau from tree-ring width. *J. Clim.* **28**, 5289–5304 (2015).
51. Yang, K. et al. Recent climate changes over the Tibetan Plateau and their impacts on energy and water cycle: a review. *Glob. Planet. Change* **112**, 79–91 (2014).
52. Tan, L. et al. Rainfall variations in central Indo-Pacific over the past 2,700 y. *Proc. Natl Acad. Sci. USA* **116**, 17201–17206 (2019).
53. Turner, A. G. & Annamalai, H. Climate change and the South Asian summer monsoon. *Nat. Clim. Change* **2**, 587–595 (2012).
54. Kraaijenbrink, P. D., Stigter, E. E., Yao, T. & Immerzeel, W. W. Climate change decisive for Asia's snow meltwater supply. *Nat. Clim. Change* **11**, 591–597 (2021).
55. Fan, H. & He, D. Temperature and precipitation variability and its effects on streamflow in the upstream regions of the Lancang-Mekong and Nu-Salween Rivers. *J. Hydrometeorol.* **16**, 2248–2263 (2015).
56. Cotterell, A. *A History of South-East Asia* (Marshall Cavendish International, 2014).
57. Hall, D. G. E. *History of South East Asia* (Macmillan International Higher Education, 1981).
58. Wolters, O. *History, Culture and Region in Southeast Asian Perspectives* (Cornell Univ. Press, 1999).
59. Aung-Thwin, M. & Aung-Thwin, M. *A History of Myanmar Since Ancient Times: Traditions and Transformations* (Reaktion Books, 2013).
60. Baran, E., Van Zalinge, N. & Bun, N. P. Floods, floodplains and fish production in the Mekong Basin: present and past trends. In *Proc. Second Asian Wetlands Symposium, 27–30 August 2001, Penang, Malaysia* pp. 920–932 (Penerbit Universiti Sains Malaysia, 2001).
61. Gundersen, L. G. A reassessment of the decline of the Khmer Empire. *Int. J. Cult. Hist.* **1**, 63–66 (2015).
62. Carter, A. K. et al. Temple occupation and the tempo of collapse at Angkor Wat, Cambodia. *Proc. Natl Acad. Sci. USA* **116**, 12226–12231 (2019).
63. Penny, D. & Beach, T. P. Historical socioecological transformations in the global tropics as an Anthropocene analogue. *Proc. Natl Acad. Sci. USA* **118**, e2022211118 (2021).
64. Penny, D. et al. The demise of Angkor: systemic vulnerability of urban infrastructure to climatic variations. *Sci. Adv.* **4**, eaau4029 (2018).
65. Bibi, S. et al. Climatic and associated cryospheric, biospheric, and hydrological changes on the Tibetan Plateau: a review. *Int. J. Climatol.* **38**, 1–17 (2018).
66. Wang, J. et al. Tree-ring inferred annual mean temperature variations on the southeastern Tibetan Plateau during the last millennium and their relationships with the Atlantic Multidecadal Oscillation. *Clim. Dyn.* **43**, 627–640 (2014).
67. Chen, F. et al. Late twentieth century rapid increase in high Asian seasonal snow and glacier-derived streamflow tracked by tree rings of the upper Indus River basin. *Environ. Res. Lett.* **16**, 094055 (2021).

[1]Yunnan Key Laboratory of International Rivers and Transboundary Eco-Security, Institute of International Rivers and Eco-Security, Yunnan University, Kunming, China. [2]Southwest United Graduate School, Kunming, China. [3]State Key Laboratory of Numerical Modeling for Atmospheric Sciences and Geophysical Fluid Dynamics (LASG), Institute of Atmospheric Physics, Chinese Academy of Sciences, Beijing, China. [4]Department of Geography, Johannes Gutenberg University, Mainz, Germany. [5]Global Change Research Institute (CzechGlobe), Czech Academy of Sciences, Brno, Czech Republic. [6]Laboratory of Tree-Ring Research, University of Arizona, Tucson, AZ, USA. [7]Department of Geography, University of Cambridge, Cambridge, UK. [8]Department of Geography, Faculty of Science, Masaryk University, Brno, Czech Republic. [9]Swiss Federal Research Institute (WSL), Birmensdorf, Switzerland. [10]Key Laboratory of Tree-ring Physical and Chemical Research, Institute of Desert Meteorology, China Meteorological Administration, Urumqi, China. [11]Laboratorio de Dendrocronología de Zonas Áridas CIGEOBIO (CONICET-UNSJ), Gabinete de Geología Ambiental (INGEO-UNSJ), San Juan, Argentina. [12]Laboratorio de Dendrocronología e Historia Ambiental, IANIGLA-CCT CONICET-Universidad Nacional de Cuyo, Mendoza, Argentina. [13]Hémera Centro de Observación de La Tierra, Escuela de Ingeniería Forestal, Facultad de Ciencias, Universidad Mayor, Huechuraba, Santiago, Chile. [14]State Key Laboratory of Vegetation and Environmental Change, Institute of Botany, Chinese Academy of Sciences, Beijing, China. [15]ALPHA, State Key Laboratory of Tibetan Plateau Earth System, Environment and Resources (TPESER), Institute of Tibetan Plateau Research (ITPCAS), Chinese Academy of Sciences, Beijing, China. [16]College of Resources and Environment, University of Chinese Academy of Sciences, Beijing, China. [17]MOE Key Laboratory of Western China's Environmental System, Lanzhou University, Lanzhou, China. [18]These authors contributed equally: Feng Chen, Wenmin Man. ✉e-mail: feng653@163.com; dmhe@ynu.edu.cn; fhchen@itpcas.ac.cn

Methods

Tree ring and streamflow data

Ten tree-ring-width site chronologies were developed from increment cores collected during the 2007–2018 field seasons, from juniper (*Sabina tibetica*), spruce (*Picea likiangensis*) and fir (*Abies forrestii*) in the southern Tibetan Plateau (Fig. 1 and Supplementary Table 1), and were used to reconstruct the September–July streamflow of the Mekong, Salween and Yarlung Tsangpo rivers. Instrumental data, 1960–2004, were obtained from stream gauge stations Chiang Saen, Nuxia and Daojieba (Fig. 1 and Supplementary Table 1) and were used to assess the covariance between the seasonal subsets of aggregated streamflow and tree-ring chronologies. NDVI data[45] were used to assess the influence of streamflow on regional vegetation growth.

Streamflow reconstructions

The reconstructions were developed using a nested principal component regression procedure[68] and included 14 separate nests linked continuously from 1000 to 2018 CE (Supplementary Table 2). A separate principal component analysis was conducted on the common periods for the proxy predictors for which complete data within a particular nested period were available. Principal components with eigenvalues >1.5 were retained as predictors for subsequent multiple linear regression (MLR) analysis.

A similar regression procedure was followed for each nested model. The full period available for model calibration was 44 years (1961–2004). A split-sample validation (with the calibration performed on the last half and validation on the first) was conducted to check the stability of the relationships and obtain validation skill statistics using a 50-year sliding window with a 25-year overlap (Supplementary Table 2). The reduction of error (RE) and R^2 statistics were used to assess the skill of each nested model[69]. The final model used for reconstruction was then calibrated using the full instrumental 1961–2004 period. The predictors input to the final model were selected by forward stepwise regression; predictors were retained if the regression coefficient differed significantly ($P < 0.05$) according to a *t*-test.

Long-term tree-ring chronologies were substituted into the regression models to generate nested reconstructions. Because some chronologies were more up to date than the available streamflow series, the reconstructions could extend the streamflow record not only into the past (year 1000), but forward to 2018, 14 years beyond the limit of the instrumental calibration streamflow data.

MLR

MLR has been widely used in detection and attribution studies[70,71]. Before the application of MLR in the CESM-LME simulation, we smoothed all independent variables using a 30-year low-pass filter and normalized the time series data to obtain a consistent mean and standard deviation with the following equation:

$$\mathrm{STR} = \beta_0 + \beta_1 \mathrm{PDO} + \beta_2 \mathrm{AMV} + \beta_3 \mathrm{STR_{GHG}}$$
$$+\beta_4 \mathrm{STR_{LULC}} + \beta_5 \mathrm{STR_{Orb}} + \beta_6 \mathrm{STR_{Sol}} + \beta_7 \mathrm{STR_{Vol}} + \beta_8 \mathrm{STR_{Aero}}$$

where STR represents the streamflow from all predictors and STR_i represents the streamflow from individual-forcing simulations. We considered PDO, AMV and six additional forcings: greenhouse gases, land use, orbital parameters, solar activity, volcanic eruptions and ozone loading. The explanatory variance (EV) of the relative contribution was calculated as follows:

$$\mathrm{EV}_i = \frac{|\beta_i| R^2}{\sum_{i=1}^{n} |\beta_i|} \times 100\%$$

Calculation of the PDO and AMV

Following the methods of Mantua et al.[72], we define the PDO index considering the first principal component of the North Pacific SST between 20° N and 60° N and between 110° E and 110° W[49,73]. The AMV index is defined as the SST difference between the North Atlantic (0°–65° N, 80° W–0°) and the global ocean[47].

Climate models

We obtained hydroclimate data of ten fully forced members and surface runoff data of six individually forced simulations from the CESM-LME, including greenhouse gases, land use types, orbital parameters, solar activity, volcanic eruptions and ozone loading. Representative Concentration Pathway 8.5 in the CESM Large Ensemble (CESM-LE)[74] is used to predict streamflow changes in the CESM models, representing solar radiative forcing of 8.5 W m^{-2} in 2100. CESM-LE was begun with a multi-century 1850 control simulation with constant pre-industrial forcing. All 30 ensemble members have the same specified external forcing, including historical forcing from 1920 to 2005 and Representative Concentration Pathway 8.5 forcing from 2006 to 2100. The model version of CESM-LE is the same as CESM-LME (CESM1). Additionally, both simulations use the same sets of forcings during the overlapping period (1920–2005), except the CESM-LME also considered the impact of orbital changes[75]. The SSP2-4.5 and SSP5-8.5 scenarios were applied to the surface runoff from 26 CMIP6 models, namely the ACCESS-CM2, ACCESS-ESM1-5, BCC-CSM2-MR, CanESM5, CAS-ESM2-0, CESM2-WACCM, CMCC-CM2-SR5, CMCC-ESM2, EC-Earth3, EC-Earth3-Veg, EC-Earth3-Veg-LR, FGOALS-f3-L, FGOALS-g3, GFDL-ESM4, INM-CM4-8, INM-CM5-0, IPSL-CM6A-LR, KACE-1-0-G, MCM-UA-1-0, MIROC6, MPI-ESM1-2-HR, MPI-ESM1-2-LR, MRI-ESM2-0, NorESM2-LM, NorESM2-MM and TaiESM1, to predict and evaluate future streamflow changes on the Tibetan Plateau. Data were integrated using the multi-model ensemble method to eliminate the uncertainty inherent in individual simulations[76,77]. Finally, to develop the model's abilities to estimate historical and future streamflows, we standardized the instrumental streamflow during the common period. Considering the linear relationship between the data series before and after this treatment, we converted the modelled runoff into historical streamflow and then scaled the future streamflow accordingly.

Data availability

The streamflow reconstruction is downloaded from the Mendeley Data Repository Center (https://doi.org/10.17632/7km7vmk4f3.1). Palaeoclimate records for comparison in Fig. 2 were obtained from the National Centers for Environmental Information (https://www.ncei.noaa.gov/access/paleo-search/?dataTypeId=18). The CESM model data can be downloaded at https://www.earthsystemgrid.org/dataset/ucar.cgd.ccsm4.CESM_CAM5_LME.html, and the CMIP data can be downloaded at https://esgf-node.llnl.gov/search/cmip6/.

Code availability

The code to carry out the current analyses is available from the corresponding authors upon request.

References

68. Meko, D. Dendroclimatic reconstruction with time varying predictor subsets of tree indices. *J. Clim.* **10**, 687–696 (1997).
69. Fritts, H. C. *Tree Rings and Climate* (Academic Press, 1976).
70. Zhou, J. & Tung, K. K. Deducing multidecadal anthropogenic global warming trends using multiple regression analysis. *J. Atmos. Sci.* **70**, 3–8 (2013).
71. Wang, J. et al. Causes of East Asian temperature multidecadal variability since 850 CE. *Geophys. Res. Lett.* **45**, 13–485 (2018).
72. Mantua, N. J., Hare, S. R., Zhang, Y., Wallace, J. M. & Francis, R. C. A Pacific interdecadal climate oscillation with impacts on salmon production. *Bull. Am. Meteorol. Soc.* **78**, 1069–1080 (1997).
73. Huang, X. et al. South Asian summer monsoon projections constrained by the interdecadal Pacific oscillation. *Sci. Adv.* **6**, eaay6546 (2020).

74. Kay, J. et al. The Community Earth System Model (CESM) Large Ensemble Project: a community resource for studying climate change in the presence of internal climate variability. *Bull. Am. Meteorol. Soc.* **96**, 1333e1349 (2015).
75. Huang, W. et al. Changes of climate regimes during the last millennium and the twenty-first century simulated by the Community Earth System Model. *Quat. Sci. Rev.* **180**, 42–56 (2018).
76. Hessl, A. E. et al. Past and future drought in Mongolia. *Sci. Adv.* **4**, e1701832 (2018).
77. Dai, A., Rasmussen, R. M., Ikeda, K. & Liu, C. A new approach to construct representative future forcing data for dynamic downscaling. *Clim. Dyn.* **55**, 315–323 (2020).

Acknowledgements

This work was supported by Basic Science Center for Tibetan Plateau Earth System (BSCTPES, NSFC project no. 41988101), the 2nd Scientific Expedition to the Qinghai-Tibet Plateau (2019QZKK010206), NSFC (91547115, 42261144687, 42075041) and Jiangsu Collaborative Innovation Center for Climate Change. J.E. and U.B. acknowledge the support of the ERC Advanced project entitled Monostar (AdG 882727).

Author contributions

F.C., D.H. and F.H.C. conceived and designed the study, with input from all other authors. F.C. and W.M. wrote the original drafts. F.C., W.M., S.W., X.Z. and M.H. performed analyses and generated all figures. All authors contributed to the discussions, reviews and improvement of this paper.

Competing interests

The authors declare no competing interests.

Additional information

Supplementary information The online version contains supplementary material available at https://doi.org/10.1038/s41561-023-01320-1.

Correspondence and requests for materials should be addressed to Feng Chen, Daming He or Fahu Chen.

Peer review information *Nature Geoscience* thanks Jianglin Wang, Matthew Therrell and the other, anonymous, reviewer(s) for their contribution to the peer review of this work. Tom Richardson, in collaboration with the *Nature Geoscience* team.